http://eprints.gla.ac.uk/83246/

Deposited on: 18 July 2013

JEM

Regulation of T cell receptor signaling by activation–induced zinc influx

Mingcan Yu,[1] Won-Woo Lee,[3] Deepak Tomar,[3] Sergey Pryshchep,[3] Marta Czesnikiewicz-Guzik,[3] David L. Lamar,[3] Guangjin Li,[1] Karnail Singh,[3] Lu Tian,[2] Cornelia M. Weyand,[1] and Jörg J. Goronzy[1]

[1]Division of Immunology and Rheumatology, Department of Medicine, and [2]Division of Biostatistics, Department of Health Research and Policy, Stanford University School of Medicine, Stanford, CA 94305
[3]Lowance Center for Human Immunology, Emory University, Atlanta, GA 30322

Zinc is a trace element that is essential for innate and adaptive immune responses. In addition to being a structural element of many proteins, zinc also functions as a neurotransmitter and an intracellular messenger. Temporal or spatial changes in bioavailable zinc may influence the activity of several enzymes, including kinases and phosphatases. We provide evidence that zinc functions as an ionic signaling molecule after T cell activation. Cytoplasmic zinc concentrations increased within 1 min after T cell receptor (TCR) triggering, in particular in the subsynaptic compartment. The increase depended on the extracellular zinc concentrations and was inhibited by silencing zinc transporter Zip6. Increased zinc influx reduced the recruitment of SHP-1 to the TCR activation complex, augmented ZAP70 phosphorylation and sustained calcium influx. By calibrating TCR activation thresholds, increased extracellular zinc bioavailability facilitated the induction of T cell proliferative responses to suboptimal stimuli.

CORRESPONDENCE
Jörg J. Goronzy:
jgoronzy@stanford.edu

Abbreviations used: mDC, myeloid DC; MFI, mean fluorescence intensity; MT, metallothionein; PTP, protein tyrosine phosphatase; SEB, staphylococcal enterotoxin B; TSST, toxic shock syndrome toxin.

Zinc is an essential trace element that is pivotal for normal immune functioning. Zinc deficiency is, in part, responsible for the compromised immune function in Third World countries, leading to increased morbidity and mortality from infections (Fischer Walker and Black, 2004). The most instructive disease is acrodermatitis enteropathica, an inherited zinc malabsorption syndrome caused by a defective zinc transporter gene, Zip4, which is necessary for intestinal zinc uptake (Küry et al., 2002). Without substitution, these patients frequently die from infections. Although complex, the immune defect preferentially involves the adaptive immune system with the key findings of thymus atrophy, lymphopenia, and compromised lymphocyte function (Fraker and King, 2004; Rink and Haase, 2007). Because of zinc's central role in immune function, supplementation is frequently advocated to improve immune health; however, the supporting evidence is mostly anecdotal (Haase et al., 2008b).

In spite of its central positioning, the mechanisms of zinc function in immune responses and, in particular, how zinc regulates T cells are unknown. Zinc is involved in many biological processes by its binding to metalloproteins. Zinc-interacting regions, such as zinc finger motifs, ring fingers, and LIM domains, have been identified in >300 different proteins including transcription factors and metalloenzymes (Vallee and Falchuk, 1993; Joazeiro and Weissman, 2000; Pabo et al., 2001; Kadrmas and Beckerle, 2004). Being an essential component of metalloproteins has been originally regarded as the sole reason for its indispensability. Indeed, zinc has important structural roles that are directly relevant for T cells. Zinc facilitates the binding of the src kinase Lck to the CD4 molecule (Kim et al., 2003) and can, therefore, be envisioned to stabilize the signaling complex important for T cell activation. CD4 brings Lck in close proximity to the TCR, thereby initiating tyrosine phosphorylation of proximal signaling molecules such as ZAP70 and CD3ζ (Kim et al., 2003).

M. Yu, W.-W. Lee, and D. Tomar contributed equally to this paper.
W.-W. Lee's present address is Dept. of Microbiology and Immunology, Seoul National University College of Medicine, Seoul 110-799, South Korea.

Supplemental Material can be found at:
http://jem.rupress.org/content/suppl/2011/03/21/jem.20100031.DC1.html

JEM

In the neurosciences, zinc is primarily considered to be an ionic signaling molecule (Frederickson et al., 2005). Zinc ions move through membrane channels among various organelles and modify the function of zinc-dependent proteins. Also, neurons have been identified that use zinc release for synaptic communication. Presynaptic terminals release zinc and post-synaptic dendrites have zinc-permeable channels, allowing for zinc transfer from inside a presynaptic to inside a postsynaptic neuron. Zinc, therefore, functions as a mediator of cell–cell signaling and acts as an autocrine or paracrine trans-membrane signaling factor.

The concept of zinc being an ionic signaling molecule has increased attention to the bioavailable zinc that is not tightly bound to proteins and is exchangeable within individual cells (Rink and Haase, 2007). Cytoplasmic zinc concentrations are influenced by cell activation and by oxidative or nitrosative stress (Maret, 2006). Undulations in free zinc ions are likely to influence signaling pathways, yielding complex interaction between zinc homeostasis and signaling. Zinc ions have been shown to inactivate tyrosine phosphatases (Haase and Maret, 2003), including the protein tyrosine phosphatases (PTPs) 1b (Eide, 2006) and PP2A (Ho et al., 2008) and serine/threonine phosphatases such as calcineurin (Aydemir et al., 2009).

The amount of intracellular and bioavailable zinc is strictly controlled by metallothioneins (MTs) and a large array of zinc transporters (Cousins et al., 2006). The expression of these molecules is cell and tissue specific and only incompletely understood for lymphoid cells. MTs bind up to seven zinc atoms by a total of 20 cysteines. Zinc can be easily released from MT under oxidative or nitrosylative stress (Kröncke et al., 2002). Zinc transporters fall into two different families. Members of the Znt or SLC30A family lower intracellular zinc by mediating zinc efflux into the extracellular fluid or influx into intracellular vesicles (Palmiter and Huang, 2004). In contrast, Zip proteins of the SLC39A family are zinc importers mediating the influx from extracellular or intracellular sources into the cytoplasm (Eide, 2004). The mammalian Znt and Zip families consist of 10 and 14 members, respectively. A variety of stimuli, including inflammatory cytokines, have been identified that control transcription of MT and zinc transporters. Activation-induced expression of MT and zinc transporters has been shown to modulate zinc homeostasis and influence immune cell function. LPS-induced induction of Znt8 reduces cytoplasmic zinc in DC and facilitates DC maturation (Kitamura et al., 2006). T cell activation up-regulates transcription of several zinc importers and of MT. Increased MT expression lowers cytoplasmic zinc (Aydemir et al., 2009), reduces reactive oxygen species (Lee et al., 2008), and is an important mechanism in T cell–proliferative responses, in particular in the elderly. Zip8 expression augments lysosomal zinc release and production of IFN-γ (Aydemir et al., 2009). Znt5 is involved in mast cell activation but not degranulation (Nishida et al., 2009).

Although evidence for zinc signaling caused by changes in transcription of zinc regulatory proteins is unequivocal, few examples have emerged to show that zinc also functions as an ionic signaling molecule similar to calcium as a result of activation-controlled transporter activity (Hirano et al., 2008; Haase and Rink, 2009). Haase et al. (2008a) have shown an immediate increase in cytoplasmic zinc in Jurkat cells after PMA and in monocytes after LPS stimulation, and Yamasaki et al. (2007) have shown this increase after FcεR1 stimulation in mast cells. In the current study, we have examined the hypothesis that zinc functions as an ionic signal in TCR-mediated T cell activation. Stimulation with superantigen presented by myeloid DC (mDC) induced a zinc influx via the Zip6 transporter from extracellular sources. Increased cytoplasmic zinc concentrations were compartmentalized in the immediate subsynaptic region and influenced the formation of the TCR activation complex by inhibiting the recruitment of SHP-1. As a consequence, zinc influx and, therefore, the extracellular zinc concentrations control signal strength and lower the TCR threshold to respond to suboptimal stimulation.

RESULTS

TCR stimulation induces zinc influx

To examine whether T cell activation modifies intracellular zinc homeostasis, CD4 T cells were labeled with the zinc ion–specific probe FluoZin-3 and stimulated with mDC loaded with the superantigens toxic shock syndrome toxin (TSST) and staphylococcal enterotoxin B (SEB). Under these conditions, $\sim$30–50% of all CD4 T cells formed an interphase with mDCs that had the characteristics of a TCR synapse with central clustering of CD3 surrounded by LFA-1 (unpublished data). FluoZin-3 mean fluorescence intensities (MFIs) in whole cells were examined at serial time points after T cells and superantigen-loaded DCs were pelleted by centrifugation. T cells that had formed a synapse were compared with T cells on the same slide that had not established contact with DC. T cells in contact with DC had increased cytoplasmic zinc concentrations. To examine whether the increase in cytoplasmic zinc was dependent on extracellular zinc, T cell stimulation with superantigen and DC was performed in 0.7 µM zinc containing RPMI supplemented with 1% FCS and $ZnCl_2$ in a concentration range of 0–75 µM. To control for equal loading of FluoZin-3, experiments in different zinc concentrations were performed in parallel with the same batch of T cells. Confocal images in Fig. 1 a were obtained 10 min after T cells and DCs were pelleted in medium containing the different zinc concentrations. Fig. 1 b shows the quantitative analysis of >50 cells for each experimental condition by displaying mean ± SEM of FluoZin-3 MFI. Nonactivated T cells not in contact with DCs had stable FluoZin-3 MFIs irrespective of the extracellular zinc concentrations. In RPMI medium not supplemented with zinc, an activation-induced increase in cytoplasmic zinc was minimal. Although these cells formed a TCR synapse, FluoZin-3 MFIs were not significantly different in stimulated and unstimulated cells (Fig. 1 b). In zinc-supplemented medium, an activation-induced increase in cytoplasmic zinc was observed. Analysis by two-way ANOVA showed a significant increase
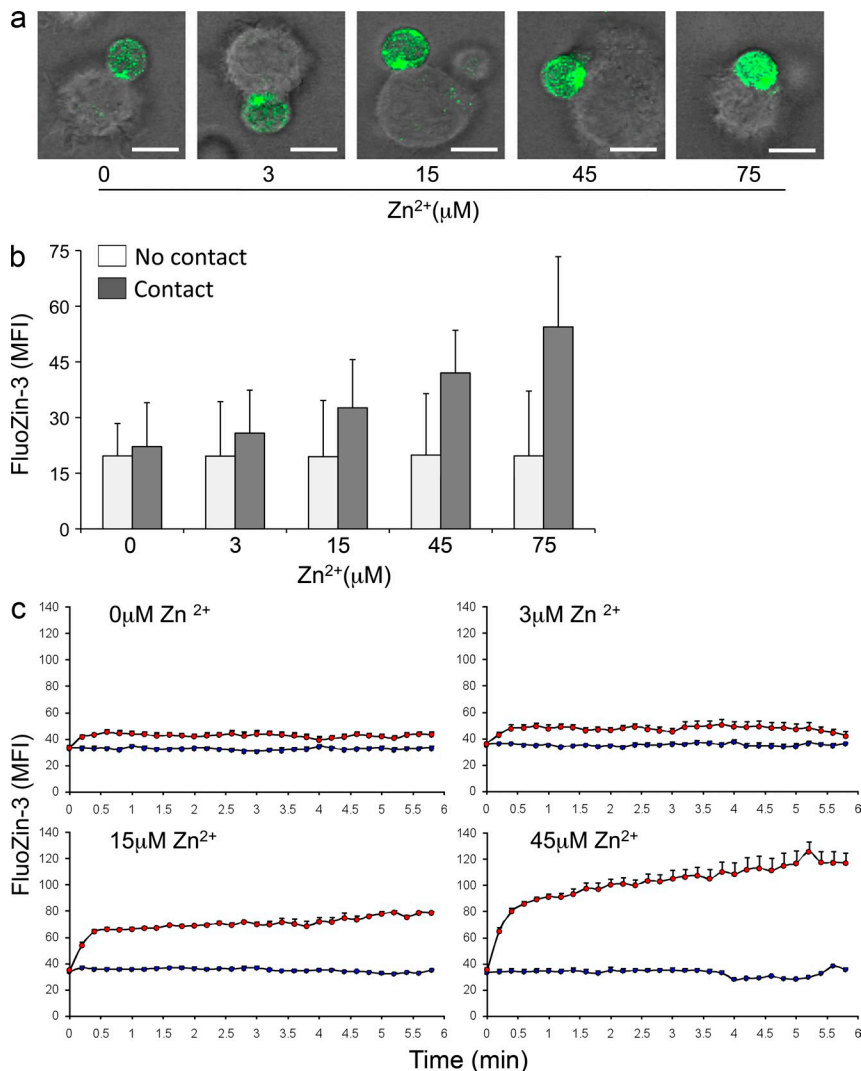
Zinc enhances T cell receptor signaling | Yu et al.

Figure 1. Activation–induced increase in cytoplasmic zinc. (a) CD4 T cells were labeled with zinc ion–specific probe FluoZin-3 AM and pelleted with TSST-1/SEB-loaded mDC by centrifugation for 1 min in RPMI medium supplemented with the indicated concentrations of $ZnCl_2$. Cells were analyzed by confocal microscopy at 10 min after centrifugation. Confocal images of representative T cell–DC clusters at increasing zinc concentrations are shown. Bars, 10 µm. (b) FluoZin-3 fluorescence was determined for CD4 T cells that had established membrane contact with DCs (shaded bars). Isolated unstimulated CD4 T cells served as control (open bars). Data are expressed as mean ± SD of MFI of >50 individual cells and are representative of three experiments. Intracellular zinc concentrations were significantly influenced by extracellular zinc concentrations ($P < 0.001$) in T cells recognizing superantigen-loaded DCs. (c) FluoZin-3–labeled CD4 T cells were cultured with TSST-1/SEB-loaded mDC RPMI medium supplemented with 0, 3, 15, and 45 µM $ZnCl_2$ and followed by live-cell imaging (12-s interval between frames). The line graphs show the tracing of T cells that were not in contact with DCs (blue line) and of T cells that had established an interaction platform with DCs (red line). Data shows the mean ± SEM of >10 individual cells and are representative of three experiments.

in intracellular zinc dependent on extracellular zinc concentration ($P < 0.001$) and contact status ($P < 0.001$). The increase in FluoZin-3 MFI ranged from ∼25% at 3 µM ($P = 0.007$) to 300% at 75 µM ($P < 0.001$). Live-cell imaging yielded similar results (Fig. 1 c). In these experiments, T cells were added to immobilized DCs and superantigen in medium supplemented with zinc and video imaged. Cells that did not establish contact with DCs displayed minor fluctuations in FluoZin-3 MFI (Fig. 1 c, blue line). An abrupt increase in cytoplasmic zinc was seen in T cells establishing contact with a DC (Fig. 1 c, red line). This increase was already seen with 3 µM zinc but was brisker and more pronounced in medium containing 45 µM.

Silencing of Zip6 prevents zinc influx

The finding that T cell activation is associated with an increase in cytoplasmic zinc dependent on extracellular zinc concentrations suggested that TCR stimulation activates a zinc transporter. Zinc influx is mediated by the family of Zip transporters that consists of 14 family members and that show

tissue-specific expression (Eide, 2004). Pilot studies to determine which Zip transcripts are expressed in unstimulated T cells identified Zip6 and Zip8 as potential candidates (unpublished data). Zip8 has been shown to be expressed in the lysosome, whereas Zip6 is a cell membrane transporter (Lichten and Cousins, 2009). Given that extracellular zinc concentrations influence activation-induced zinc homeostasis, we focused on Zip6. To repress Zip6 expression, T cells were transfected with small interfering (si) RNA using nucleofection and subsequently rested for 48 h. Control T cells were transfected with scrambled siRNA. Zip6 silencing reduced transcript numbers by >70% (Fig. 2 a). Western blots showed ∼50% reduction in protein expression. Transfected T cells were loaded with FluoZin-3, pelleted with TSST- and SEB-loaded DC in medium containing 45 µM zinc, and examined by confocal microscopy. Results are shown in Fig. 2 b. In the control transfected T cells, increased cytoplasmic zinc concentrations were observed. Zip6 silencing reduced the increase in FluoZin-3 MFI by ∼50% ($P = 0.02$). These data suggested that T cell stimulation activates the zinc transporter Zip6 leading to influx of zinc from extracellular sources. Zip6 silencing had functional consequences. In CD4 T cells cultured with DC and TSST for 24 h, the induction of the activation markers CD69 and CD25 was influenced by the zinc concentration in the culture medium (Fig. 2 c). At low zinc
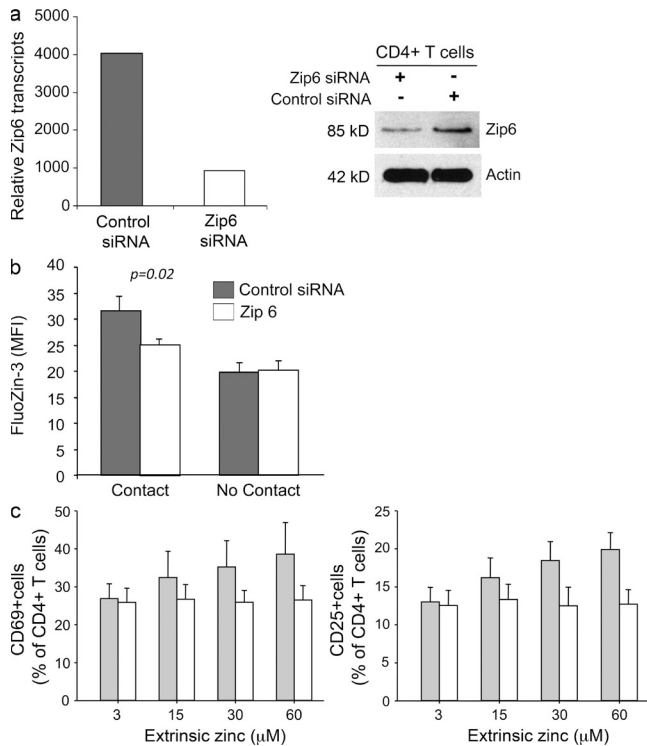
Figure 2. Activation–induced zinc influx is mediated by the zinc transporter Zip6. (a, left) CD4 T cells were transfected with scrambled control siRNA (gray bars) or with Zip6 siRNA (open bars). Zip6 mRNA was quantified 48 h after transfection by quantitative PCR. Zip6 transcripts normalized to β-actin transcripts are representative of three experiments. (a, right) Zip6 protein in control and specifically transfected T cells were detected by Western blotting. (b) On day 2 after transfection, T cells were labeled with FluoZin-3 AM and pelleted with TSST-1/SEB-loaded mDC in medium supplemented with 45 µM zinc. MFI was obtained for individual T cells that were or were not in contact with DC by confocal microscopy 10 min after 1 min of centrifugation. Results are expressed as mean ± SEM of >100 cells and are representative of three experiments. Zip6 silencing reduced the increase in FluoZin-3 MFI by ~50% (P = 0.02). (c) CD4 T cells transfected with control or Zip6 siRNA were stimulated with TSST-1 and mDC for 24 h. Frequencies of CD25- and CD69-expressing cells were determined by flow cytometry. Data are shown as mean ± SEM of four experiments.

concentrations, ~10% of all T cells was induced to express CD25, a proportion which corresponds to the frequencies of TSST-responsive Vβ2 T cells. A higher frequency was activated with increasing zinc concentrations based on nonparametric trend test (P < 0.01). The influence of zinc was no longer seen when Zip6 expression was silenced (P-value of the trend test = 0.31). Similar results were seen with CD69 expression, which is more easily induced in a higher frequency of cells. A significantly higher frequency was activated with increasing zinc concentrations (P < 0.001), and the influence of zinc disappeared when Zip6 expression was silenced (P = 0.85). Zip6 silencing inhibited T cell activation, as determined by CD69 expression, already at a concentration of 15 µM which is within the physiological range in human serum (Maret and Sandstead, 2006).
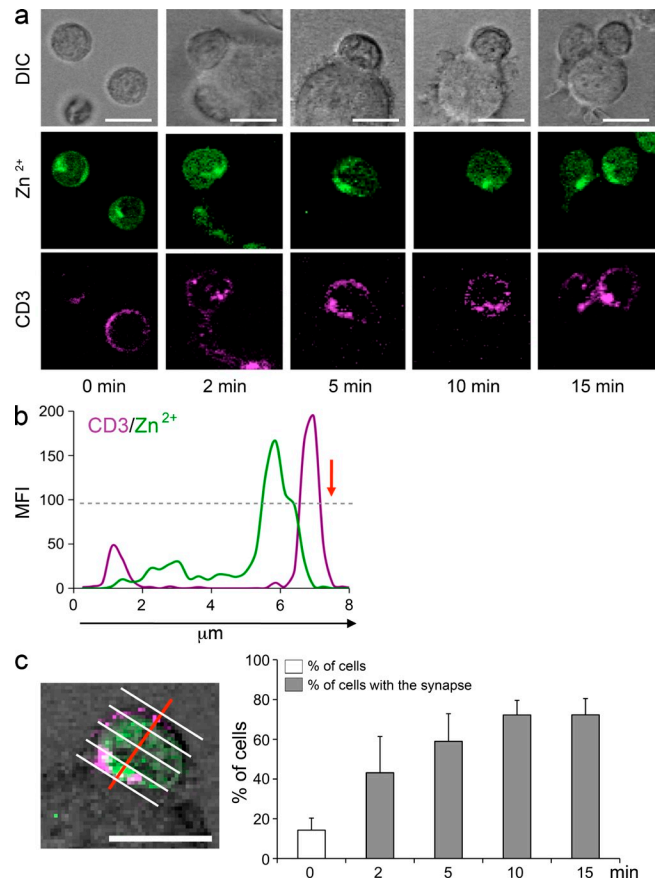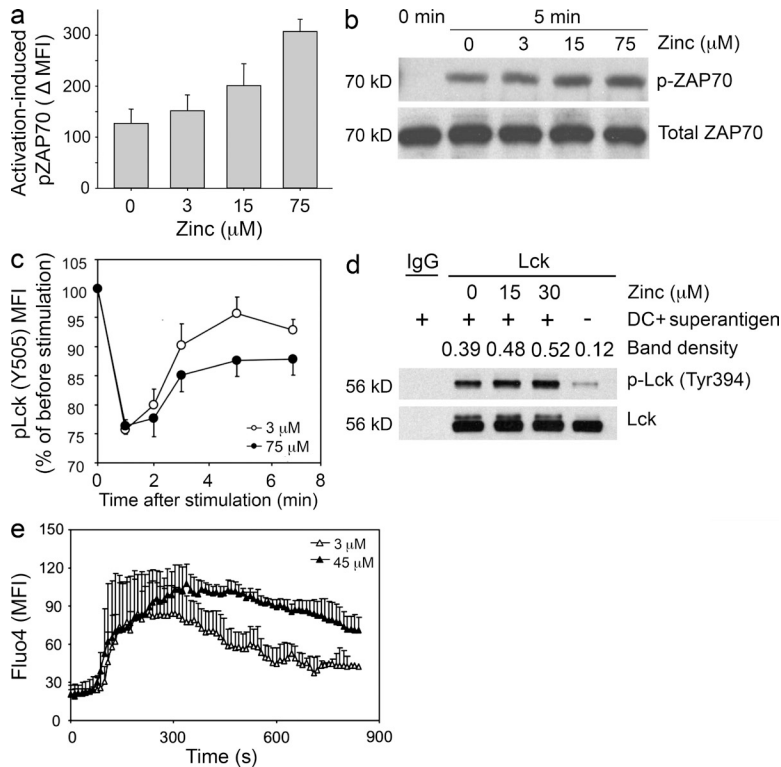

Figure 3. Subsynaptic accumulation of cytoplasmic zinc. (a) FluoZin-3–labeled CD4 T cells (green) were stained with anti-CD3 mAb (APC, purple), pelleted with TSST-1/SEB-loaded DC by centrifugation, and analyzed by confocal microscopy. DIC (top row) confocal images, FluoZin-3 fluorescence (middle row), and CD3 (bottom row) of representative T cells that had established contact with a DC are shown. Unstimulated isolated T cells (left) showed a patchy dispersed distribution of FluoZin-3 fluorescence (green). In CD4 T cells that had established a synapse with DCs, the green fluorescence was clustered in the subsynaptic region directly adjacent to the clustered CD3 molecules. (b) The image shows FluoZin-3 and CD3 fluorescence along a cross section perpendicular to the synapse (red arrow) through an individual T cell in contact with a DC 10 min after stimulation. (c) T cells were divided into quartiles parallel to the synaptic interphase (perpendicular to the red line) and FluoZin-3 MFIs were determined for each quartile. Subsynaptic accumulation of cytoplasmic zinc was defined as greater than twofold FluoZin-3 fluorescence intensities in the quartile next to the contact area compared with the distal quartile. Frequencies of T cells with accumulation of cytoplasmic zinc at indicated time points after stimulation are shown based on the analysis of >20 T cells forming a synapse with a DC (closed bars). Results are shown as mean ± SD frequencies obtained from four visual fields. FluoZin-3 fluorescence accumulation in a given quartile was found in 14% of isolated T cells not in contact with a DC (open bars). T cell stimulation significantly induced zinc sequestration in the subsynaptic region (P < 0.001). One experiment representative of four is shown. Bars, 10 µm.

Subsynaptic accumulation of cytoplasmic zinc

The increase in cytoplasmic zinc was not diffuse but compartmentalized. FluoZin-3 fluorescence in unstimulated

Figure 4. Activation–induced zinc influx augments TCR signaling. (a) CD4 T cells were stimulated for 5 min by copelleting with TSST/SEB-loaded DC in medium supplemented with 0, 3, 15, and 75 μM zinc. Phosphorylated ZAP70 levels in cell conjugates were quantified by Phosflow. Activation-induced increases in pZAP70 MFI are shown as mean ± SEM of three experiments. (b) Cell lysates from stimulated CD4 T cells were analyzed for pZAP70 by Western blotting. Membranes were stripped and reprobed for total ZAP70. One experiment representative of three is shown. (c) PBMCs were activated by CD3/CD28 cross-linking in medium supplemented with 3 μM (open circles) and 75 μM (closed circles) zinc. Cells were fixed at indicated time points, barcoded with different concentrations of Alexa Fluor 488–NHS, and analyzed for pLck (Y505). Results are shown as the pLck MFI in stimulated CD4 T cells as compared with unstimulated cells and represent mean ± SEM of seven experiments. (d) CD4 T cells were pelleted with TSST and DC in medium supplemented with 0, 15, and 30 μM zinc, incubated for 10 min, and lysed. Lck immune precipitates were analyzed for Y394 phosphorylation by Western blotting. One experiment representative of three is shown. (e) Fluo-4–labeled CD4+ T cells were co-cultured with DC pulsed with 10 ng/ml TSST-1 and 10 ng/ml SEB in medium supplemented with 3 μM (open triangles) and 45 μM (closed triangles) zinc. Fluo-4 fluorescence indicative of cytoplasmic calcium was monitored by live-cell imaging in individual cells that had established contact with a DC. Data are shown as mean ± SEM of 10 T cells and are representative of three independent experiments.

CD4 T cells that were not in contact with DC were scattered throughout the cytoplasm in a patchy distribution, which is consistent with the previous description of zincosomes in other cell types (Eide, 2006). As already evident in Fig. 1 a, increased zinc concentrations after activation clustered in the region adjacent to the TCR synapse. This clustering was already seen at low concentrations of 3 μM zinc and was maximal at 45 μM. Representative confocal images in Fig. 3 a show the FluoZin-3 fluorescence clustering in T cell–DC conjugates analyzed at serial time points after T cells, DCs, and superantigen were copelleted in medium containing 45 μM zinc. As shown in the tracing of FluoZin-3 and CD3 fluorescence along the cross section perpendicular to the synapse plane, increased cytoplasmic zinc levels colocalized with the CD3 cluster and extended into the immediate subsynaptic cytoplasmic region (Fig. 3 b). To quantitatively examine the hypothesis that zinc concentrations are elevated in the subsynaptic region, cells were dissected into quartiles along the perpendicular line (Fig. 3 c). Subsynaptic zinc clustering was defined as a twofold higher FluoZin-3 fluorescence in the synapse-close compared with the synapse-distal quartile. In unstimulated T cells, zinc clusters in a predefined quartile were found in 14% of all cells (Fig. 3 c). The percentage was significantly higher in T cells exhibiting a CD3 accumulation at the interface between T cell and DC at 2 min (P < 0.001) and 5 min (P < 0.001) after centrifugation and plateaued at 10–15 min.

Zinc functions as an ionic signaling molecule

The local accumulation of free zinc ions in the subsynaptic region raised the possibility that ionic zinc modifies early TCR signaling events. CD4 T cells were pelleted with mDCs and the superantigens SEB and TSST in medium supplemented with 0, 3, 15, and 75 μM zinc. Cells were fixed after 5 min, and phosphorylation of ZAP70 in T cell–DC conjugates was determined by Phosflow (Fig. 4 a). A nonparametric trend test was used to test the association between the activation-induced pZAP70 and zinc concentration. The null distribution was generated by randomly permuting the zinc concentration levels. The higher activation-induced pZAP70 was statistically significantly associated with the higher zinc concentration level (P < 0.001). A similar zinc-dependent increase in ZAP70 phosphorylation was seen with Western blot analysis of T cells stimulated in different zinc concentrations (Fig. 4 b), supporting the notion that zinc influx into the subsynaptic region regulates proximal signaling.

Monitoring of Lck phosphorylation at position Y505 by Phosflow after TCR stimulation provided further evidence for this notion (Fig. 4 c). As expected, inactive Y505-phosphorylated Lck changed significantly after activation over time (P < 0.001 by two-way repeated measure ANOVA); the kinetics was significantly different in medium supplemented with 3 and 75 μM zinc (P < 0.005). In the first minute after activation, inactive Lck decreased by ∼25% independent of the external zinc concentration. In medium containing 3 μM zinc, inactive Lck recovered to a plateau of ∼5% below

pretreatment levels between 2 and 7 min. This recovery was blunted with higher concentrations of zinc in the medium. Lck phosphorylation in medium supplemented with 3 and 75 µM zinc differed significantly at 5 min (P = 0.004 by post-hoc comparison with Tukey's test), whereas no difference was seen at 1 min and a trend that did not reach significance was evident at 2 and 7 min. To directly confirm a zinc-dependent increase in Lck activation, T cells were pelleted with DCs and the superantigens TSST and SEB in medium supplemented with 10% FCS and 0, 15, and 30 µM zinc, cells were lysed, and Lck was immunoprecipitated after 10 min of co-culture and examined for Y394 phosphorylation by Western blotting. Y394-phosphorylated Lck correlated with the zinc concentrations in the culture medium (Fig. 4 d). These data suggest that zinc inhibits a negative-feedback loop. This interpretation was supported by monitoring cytoplasmic calcium by live-cell imaging. CD4 T cells were labeled with Fluo-4 and co-cultured with TSST/SEB-loaded mDC. Fluo-4 fluorescence intensity, which is indicative of cytoplasmic calcium concentrations, was monitored in individual T cells that established contact with DC (Fig. 4 e). Cytoplasmic calcium showed an abrupt increase that was initially not different for cells cultured in medium containing 3 or 45 µM zinc. About 2–2.5 min after the initial calcium increase, the Fluo-4 curves in CD4 T cells that were cultured in 3 and 45 µM zinc diverged. Increased calcium concentrations declined in the T cells exposed to the low zinc concentrations, whereas in T cells cultured in 45 µM zinc calcium concentrations were increased for the entire observation period.

To examine the mechanisms by which zinc influx modifies TCR signaling, we first examined the hypothesis that increased zinc supports the recruitment and binding of Lck to CD4 or CD8, which is known to be zinc dependent. CD4 T cells were pelleted with DC at a ratio of 5:1 and with 10 ng/ml TSST and 10 ng/ml SEB in RPMI/10% FCS supplemented with 0, 15, or 30 µM zinc. After 10 min, the TCR complex was immunoprecipitated using anti-TCR antibodies,

and the precipitate was probed for the quantity of Lck. No increase in Lck recruitment to the TCR activation complex was seen with increasing extracellular zinc concentrations at the time of stimulation (Fig. 5 a). Alternatively, increased zinc influx may prevent the activation of negative-feedback loops. TCR precipitates were probed for the presence of SHP-1 (Fig. 5 b). Extracellular zinc concentration inversely correlated with reduced SHP-1 in the TCR activation complex subsequent to superantigen-mediated stimulation, suggesting that zinc influx regulates the recruitment of SHP-1.

Zinc tunes TCR activation threshold

Results so far have indicated that upon TCR stimulation, local zinc ion concentrations in the subsynaptic region increase inhibition of the negative-feedback loop exerted by SHP-1 recruitment and lead to increased ZAP70 phosphorylation and sustained Lck and calcium signals. As the signal amplification mediated by ERK activity has been shown to act through inhibiting SHP-1 recruitment and is of functional importance for discriminating between agonistic and antagonistic peptides, extracellular zinc concentrations should control TCR tuning and facilitate T cell responses to suboptimal stimulation or to low-affinity antigens. To examine this hypothesis, CFSE-labeled CD4 T cells were stimulated with suboptimal concentrations of cross-linked anti-CD3/anti-CD28 antibodies in medium containing increasing concentrations of zinc supplementation and examined on day 4 by flow cytometry. The frequencies of T cells that responded to the suboptimal stimulation and underwent at least one division were influenced by the zinc concentration (P < 0.001 by ANOVA) and increased about fivefold from ∼5 to 25% (Fig. 6 a). In the pairwise comparisons (Tukey test), statistically significant differences were seen in the concentration range between 3 and 30 µM zinc but not by comparing 30 to 45 or 75 µM zinc.

In a second system, CFSE-labeled CD4 T cells were stimulated with DC and TSST. In this system, Vβ2+ T cells represent high-affinity responders to TSST and are activated. In contrast, Vβ2− cells only bind to TSST with low affinity and are usually not stimulated. CFSE blots from a representative experiment are shown in Fig. 6 b. Almost all Vβ2+ T cells were activated by TSST-pulsed DCs, irrespective of the zinc media concentration. Higher zinc concentrations slightly accelerated cell divisions. The results were more striking for Vβ2− T cells. Only a very few of these cells were activated and entered cell cycle in medium containing 3 µM zinc. In contrast, an increased frequency of Vβ2− T cells proliferated with 15 and 75 µM zinc. Results from 11 experiments are summarized in Fig. 6 c. Compared with 3 µM zinc, the frequency of Vβ2− cells having entered the cell cycle was increased by ∼20% in medium supplemented with 15 µM zinc (P < 0.004) and by ∼50% in medium supplemented with 75 µM zinc (P < 0.001).

To examine TCR tuning by zinc in a defined antigen-specific system, 3L2 TCR transgenic mice specific for the hemoglobin peptide Hb_{64-76} were used. Splenocytes were labeled with CFSE and stimulated with 1 and 10 µM Hb_{64-76} peptide (GKKVITAFNEGLK) in different zinc concentrations
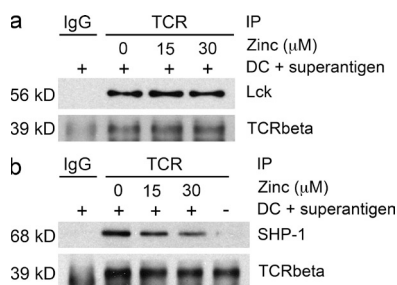

Figure 5. Zinc influx regulates SHP-1 recruitment to the TCR activation complex. CD4 T cells were stimulated with TSST and DC for 10 min in medium supplemented with 0, 15, and 30 µM zinc (lanes 2–4). Unstimulated T cells were included as control (lane 5). The TCR activation complex was immunoprecipitated with TCR-specific antibodies and the precipitate was probed for the amount of TCR-β chain, Lck (a), and SHP-1 (b) by Western blotting. Precipitation with secondary antibodies only was used as a control (lane 1). One experiment representative of three is shown.
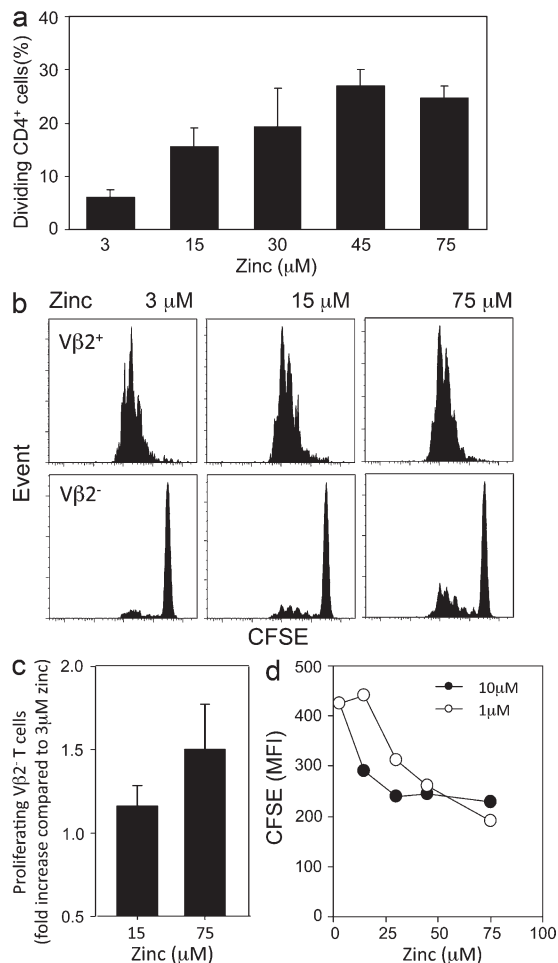
Figure 6. Zinc tunes TCR activation threshold. (a) CFSE-labeled CD4 T cells were stimulated with suboptimal concentrations of plate-bound anti-CD3/anti-CD28 antibodies in medium supplemented with $ZnCl_2$ as indicated. CFSE histograms were used to determine the percentage of CD4 T cells that had entered cell cycle and divided. Results are representative of seven experiments and are shown as mean ± SD of quadruplicate wells. (b) CFSE-labeled CD4+CD45RA+ naive T cells were stimulated with mature DC and 0.04 ng/ml of TSST-1 at indicated zinc concentrations. Representative CFSE histograms of TCR Vβ2-positive and -negative CD4 T cells are shown. (c) The fraction of TSST low-avidity Vβ2− T cells that had entered cell division was determined. Data obtained with medium containing 15 and 75 µM zinc are expressed relative to the results obtained with 3 µM zinc and are shown as mean ± SD of 11 experiments. (d) 3.L2 TCR transgenic mouse splenocytes were labeled with CFSE and stimulated with 1 and 10 µM Hb_{64-76} peptide in zinc-supplemented medium. Results are shown as CFSE MFI on day 5 and are representative of three experiments.

(Fig. 6 d). Increased zinc concentrations accelerated the proliferative response to 1 µM, as well as to 10 µM, of peptide. At zinc concentrations of 3 µM, 10 µM of peptide stimulated more efficiently than 1 µM. In contrast, a lesser difference between the different peptide concentrations was seen at concentrations of 30 µM zinc and higher. These data showed that the increased zinc influx compensated for the lower peptide concentration and optimized the response.

DISCUSSION

In this manuscript, we provide evidence that zinc functions as an ionic signaling molecule after T cell activation. Cytoplasmic zinc concentrations increased within 1 min after TCR triggering as the result of an influx via the zinc transporter Zip6. The increase was most pronounced in the immediate subsynaptic area and enhanced TCR signaling, at least in part as a result of inhibition of SHP-1 recruitment. Consequently, TCR activation thresholds were lowered and T cell responses were induced under suboptimal conditions.

Zinc's function as a novel second messenger/signaling ion has been predicted to be of similar importance to the well established role of calcium ions (Frederickson et al., 2005; Rink and Haase, 2007). Two different categories of intracellular zinc signaling have been identified. The first one depends on transcriptional changes in zinc transporter expression. This mechanism has been described in DC after LPS stimulation, which induces the expression of zinc exporters, lowers cytoplasmic zinc, and facilitates DC maturation (Kitamura et al., 2006). A similar mechanism is also functional in T cells where increased expression of zinc importers 48–72 h after TCR stimulation increases cytoplasmic zinc concentrations. Zinc influx mediated by increased transcription of Zip6 induces the expression of MTs, which supports T cell proliferation and is of particular importance for T cell survival and expansion in the elderly (Lee et al., 2008). Increased expression of Zip8 after T cell stimulation induces increased release of lysosomal zinc blocking calcineurin activity and increasing IFN-γ transcription (Aydemir et al., 2009). In contrast, a direct effect of cell activation on zinc homeostasis has been shown for mast cells, where cross-linking of the high-affinity IgE receptor induces release of free zinc from the perinuclear area (Yamasaki et al., 2007). This increase in cytoplasmic zinc was coming from intracellular sources and depended on a calcium signal as well as activation of the Ras–MAPK pathway. Also, Kaltenberg et al. (2010) showed that activation of the ERK pathway after IL-2 receptor stimulation was zinc dependent, presumably as a result of inhibition of phosphatase activity. In our study, a change in intracellular zinc concentration was observed within 1 min after T cell activation, documenting a direct effect on transporter activity. In contrast to the study by Yamasaki et al. (2007), the increase in cytoplasmic zinc was dependent on extracellular sources and correlated to the concentration of zinc in the medium. The increase in cytoplasmic zinc was largely prevented by depleting zinc from the medium or by silencing the Zip6 transporter that is expressed in the cytoplasmic membrane.

Surprisingly, the increased zinc concentrations were mostly confined to the subsynaptic area of the T cell–DC interaction platform (Figs. 1 a and 3 a). This pattern is in stark contrast to the activation-induced influx of calcium ions, where waves of increased calcium concentrations readily spread throughout the cell. One possible explanation for this pattern is that TCR activation induces clustering and activation of Zip6 transporters in the synaptic region consistent with the dependency of subsynaptic zinc accumulation on extracellular

zinc concentrations. However, a contribution from intracellular sources cannot be excluded. For calcium, release from intracellular stores is required for propagating and sustaining the signal. In activated T cells, zinc is released from lysosomes via a Zip8–dependent mechanism. Zip8 is expressed in resting T cells, although it is largely up-regulated after activation, a pattern which it shares with Zip6. Staining with Lysotracker showed accumulation of lysosomes in the subsynaptic region colocalizing with increased FluoZin-3 fluorescence (unpublished data). In this model, Zip6-dependent zinc influx from extracellular sources after T cell activation cooperates with redistribution of lysosomes and zinc release to build a steep gradient of zinc concentration in the subsynaptic region that influences proximal TCR signaling.

Early events in TCR signaling are tyrosine phosphorylations of several signaling molecules. The src protein kinase Lck is primarily responsible for the early phosphorylation events of tyrosines within the ITAM motifs of CD3ζ and ZAP70 (Palacios and Weiss, 2004). Data in Fig. 4 show that extracellular zinc influences ZAP70 phosphorylation. Lck is bound to CD4 or CD8. In fact, the sequestration of Lck by CD4 or CD8 has been identified as the major mechanism imposing a MHC class I or II restriction on T cell responses (Van Laethem et al., 2007). This binding of Lck to CD4 or CD8 is dependent on zinc, suggesting that zinc functions as a structural element in synapse formation. However, our studies did not confirm the hypothesis that zinc influx is important in CD4-Lck binding. Immune precipitation studies of the TCR activation complex did not demonstrate an influence of extracellular zinc concentrations on Lck recruitment to the TCR synapses (Fig. 5 a).

Our studies show that inhibition of negative regulatory feedback loops account at least in part for the increased ZAP70 phosphorylation. A prime candidate is SHP-1, which has been shown to be recruited to Lck and then to dephosphorylate tyrosines within ITAM motifs of ZAP70 and other signaling molecules (Altan–Bonnet and Germain, 2005). In our immune precipitation studies, recruitment of SHP-1 to the TCR synapse was reduced by increasing zinc influx. It is possible that zinc induces steric conformation changes in SHP-1 that prevent binding to Lck. Alternatively, increased ERK activity as a result of phosphatase inhibition may cause serine phosphorylation of Lck that prevents SHP-1 binding. We and others have shown that the dual-specific phosphatase DUSP6 is involved in TCR threshold calibration by increasing ERK activity (Li et al., 2007), and DUSP activity has been shown to be sensitive to zinc concentrations (Junttila et al., 2008).

It cannot be excluded that in addition to reduced SHP-1 recruitment, direct modulation of phosphatase or kinase enzyme activities by zinc also contributes to the increased signaling. Supplementation of cell lysates with 5–20 µM zinc yielded free zinc concentrations in the physiological nanomolar range and dose-dependently suppressed total phosphatase activity (Kaltenberg et al., 2010), suggesting that zinc fluctuations in space and time regulate phosphorylation signals. In vitro, SHP-1 has an IC50 of 93 nM (Haase and Maret, 2003),

which may be achieved by the local gradient in the subsynaptic region. In addition, zinc may influence the regulation of Lck activity by phosphorylation of inhibitory tyrosines in the C terminus at position Y505 (Mustelin and Burn, 1993). The balance between active and inactive Lck is maintained by the PTP CD45 and the kinase Csk. Whereas CD45 dephosphorylates Lck Y505, Csk rephosphorylates Lck at this position (Mustelin et al., 2005). Activity of Csk is regulated by two mechanisms. The compartmentalization of Csk is determined by its binding protein that recruits Csk to the cell membrane (Rahmouni et al., 2005). Upon T cell activation, Csk binds to the phosphoprotein G3bp, which is situated in an intracellular location adjacent to the immune synapse and, therefore, is presumed to exclude Csk from the initial signaling complex. Lck phosphorylates the cell membrane protein Cbp/PAG, which then recruits Csk to the synapse leading to the inactivation of Lck. Csk kinase activity has been shown to be magnesium dependent and inhibited by zinc (Sun and Budde, 1999). This inhibition occurs in nanomolar range and is reversible. In addition to its phosphorylation of the C terminus–negative regulatory tyrosine, Csk also affects Lck activity by recruiting PTPN22, which dephosphorylates the positive regulatory tyrosines on Lck. PTPs have been shown to be particularly sensitive to the inhibitory action of zinc ion (Haase and Maret, 2005). The classical example is PTP1B, which is inhibited by zinc in vitro at an IC50 of 17 nM, a concentration which is likely to be achieved in vivo. Data on the zinc sensitivity of PTPN22 are not available, but inhibition of both Csk and PTPN22 could contribute to the sustained Lck activation that we have observed with increased zinc influx.

Zinc influx was seen in in vitro systems that closely mimicked physiological activation. We used a DC–superantigen system to stimulate peripheral blood CD4 T cell, which allowed us to study the influx of zinc and signaling events in the context of TCR synapse formation. If T cells were activated by pharmacological stimulation such as CD3/CD28 cross-linking, zinc influx and associated signaling modifications were less evident, emphasizing the importance of physiological synapse formation (unpublished data). We used a large range of zinc concentrations from 3 µM to supraphysiological concentrations of 45 and 75 µM in RPMI supplemented with 10% serum. Bioavailable free zinc linearly correlated with total zinc in our culture system over the entire dose range (Fig. S1). Physiological zinc serum concentrations are ~15 µM, and zinc deficiency is defined as a serum level of <10.7 µM (Lichten and Cousins, 2009). The relevant zinc concentrations in biological compartments are unknown, and serum zinc concentrations are poor biomarkers of the zinc status (Lichten and Cousins, 2009). In all of our assay systems, results directly correlated with zinc concentrations in the medium, and effects were consistently seen at <30 µM, suggesting that activation–induced ionic zinc signaling is physiologically relevant. In most experiments, effects leveled off at concentrations of >30–45 µM zinc.

In the functional studies, increased zinc influx lowered the threshold to TCR stimulation, which is consistent with the concept that the local cytoplasmic accumulation of zinc inhibits a negative-feedback mechanism in TCR signaling. Proliferative T cell responses under suboptimal antigen conditions were improved by higher media concentration of zinc. We used several systems to examine this hypothesis. Results in all systems were consistent. Higher extracellular zinc concentrations increased the proliferative responses to suboptimal anti-CD3 stimulation. In the more physiological system, we used naive T cells, mDCs, and the superantigen TSST. Under normal conditions, TSST only activates $V\beta2^+$ cells. However, under optimized conditions, small numbers of $V\beta2^-$ T cells, which presumably have a low affinity to TSST, are also activated by the superantigen. Increased medium concentration of zinc allowed for the stimulation of $V\beta2^-$ T cells, suggesting that zinc facilitates a low avidity T cell response. Finally, increased concentrations could compensate for lower antigen peptide concentrations in an antigen-specific response using naive T cells from TCR transgenic mouse and the appropriate peptide antigen. This increased responsiveness is explained by a decreased recruitment of SHP-1 to the TCR activation complex. Interestingly, increased zinc concentrations could not restore the immune response to an antagonistic peptide (unpublished data), although the negative regulatory feedback mechanism by SHP-1 has been implicated in the tolerance induction by antagonistic peptides (Altan-Bonnet and Germain, 2005). Apparently, zinc influx is sufficient to improve TCR signaling but not to a degree that interferes with tolerance mechanisms.

We propose a model where influx of zinc after TCR stimulation leads to a local increase in cytoplasmic zinc, modifies early TCR signaling events, and selectively lowers TCR activation thresholds. The local confinement of increased zinc concentrations targets the effect to amplifying proximal TCR signals without globally modifying the many different cellular processes regulated by zinc-binding proteins. Because the zinc influx originates from extracellular sources, local manipulation of zinc availability may be a means to enhance T cell responses to antigens or vaccines. A target of particular interest is the zinc importer Zip6, which accounts for the zinc influx during T cell activation.

MATERIALS AND METHODS

Cell preparation. Peripheral blood was obtained from healthy adult volunteers after informed consent. The study was approved by the Emory and Stanford University Institutional Review Boards. CD4 T cells were isolated from whole blood using a human CD4 T cell enrichment cocktail kit (RosetteSep; STEMCELL Technologies). Naive CD4 T cells were further isolated by positive selection with anti-CD45RA magnetic beads (Miltenyi Biotec). PBMCs were purified by gradient centrifugation with Ficoll. Monocytes were purified from PBMCs by AutoMACS using anti-CD14 magnetic beads (Miltenyi Biotec) and cultured in RPMI 1640 supplemented with 10% FCS, 800 U/ml GM-CSF, and 1,000 U/ml IL-4 (R&D Systems) to generate mDCs. On day 6, mDCs were harvested and matured with 1,100 U/ml TNF (R&D Systems) and 1 µg/ml PGE$_2$ (Sigma-Aldrich) for 24 h.

Proliferation assays. 25×10^3 CD4 naive T cells labeled with CFSE were co-cultured with 500 matured mDCs and 0.04 ng/ml TSST-1 (Toxin Technology, Inc.) in RPMI 1640/10% FCS supplemented with ZnCl$_2$ to the final

concentrations of 3, 15, 30, 45, and 75 µM zinc. Free zinc in the medium was determined by using the zinc probe FluoZin-3 (Invitrogen) as previously described (Kaltenberg et al., 2010). About 50% of the zinc was bioavailable over the entire concentration range, suggesting that the binding capacity of the serum was not limiting (Fig. S1). On day 4 after stimulation, the cells were harvested and stained with PE-conjugated anti-TCR Vβ2 (Beckman Coulter), and CFSE dilution in V$\beta2^+$ or V$\beta2^-$ CD4$^+$ naive T cells was assessed using an LSRII (BD).

In some experiments, CFSE-labeled CD4 T cells were stimulated for 6 d on plates coated with 1 µg/ml anti-CD3 antibody (OKT3; Ortho Clinical Diagnostics) and 1 µg/ml anti-CD28 (clone CD28.2; BD). CFSE-labeled splenocytes from 3.L2 TCR transgenic mice (provided by B. Evavold, Emory University, Atlanta, GA) were stimulated at a concentration of 3×10^5 per 200 µl with 1 or 10 µM of the hemoglobin Hb$_{64-76}$ peptide in RPMI/10% FCS supplemented with ZnCl$_2$. CFSE profiles were determined on day 5.

Confocal studies. CD4 T cells were stained with anti–human CD3 antibody (BD) labeled with Alexa Fluor 555 mouse IgG$_1$ (Invitrogen) at 4°C and subsequently with FluoZin-3 AM (Invitrogen) at 37°C. To control for FluoZin-3 loading, T cells were incubated with 5 µM pyrithione in the presence of medium containing 75 µM zinc, and the increase in whole cell fluorescence was determined (Fig. S2 a). Conversely, the decrease in fluorescence in cells treated with 0.1% Triton X-100 was monitored (Fig. 2 b). Mature mDCs were preincubated with 10 ng/ml TSST and 10 ng/ml SEB (Toxin Technology, Inc.) for 30 min. 3×10^5 CD4 T cells were pelleted with 1×10^5 mDCs and superantigen in zinc-supplemented medium by centrifugation for 1 min at 1,350 rpm (400 g) and imaged at the indicated time points after centrifugation. All images were collected using a Plan-Apochromat 63×/1.4 NA oil differential interference contrast (DIC) objective. Image capture was done with a confocal laser-scanning microscope (LSM 510 META inverted Axiovert 200; Carl Zeiss). Samples were illuminated with both the 488- and 543-nm laser lines from the Argon/Helium Neon laser. Images were collected as vertical Z-stacks and projected in three dimensions or subsampled for the dish plane. Image analysis was performed using the public domain software ImageJ (http://rsb.info.nih.gov/ij) and LSM-510 Expert Mode software (Carl Zeiss). Results are shown as MFI of whole cells subtracted by background MFI. T cells that had formed a synapse with DCs as indicated by CD3 clustering in the contact area, and T cells that had not formed conjugates with DCs were compared. A minimum of 50 T cells per condition was analyzed.

For live-cell imaging, mDCs were matured with TNF and PGE$_2$ on poly-L-lysine glass-bottom culture dishes (MatTek Corporation) for 24 h. CD4 T cells were labeled with FluoZin-3 AM or with Fluo-4 AM to assess cytoplasmic zinc or calcium concentrations and then added to the DC cultures at a cell ratio of 10:1 in the presence of 10 ng/ml TSST-1 and 10 ng/ml SEB (Toxin Technology, Inc.). Video images were recorded using the LSM 510 META inverted Axiovert-200M microscope. All images were collected using a Plan-Apochromat 63×/1.4 Oil DIC objective. To estimate [Ca^{2+}]i and [Zn^{2+}]i, MFIs were determined for individual whole cells from four focal z-slices.

Quantitative PCR. Total RNA was isolated from purified CD4 naive and memory T cells using TRIzol (Invitrogen). cDNA templates were synthesized using the First Strand cDNA Synthesis kit for RT-PCR (Roche). Quantitative PCR was performed on an Mx3000 qPCR system (Agilent Technologies) with the following primer sets: Zip6, 5′-GATGGTGATAATGGGTGAT-3′ and 5′-CCAGCCTTTAGTAGAACAG-3′, annealing temperature 55°C and 18s; and 5′-AGGAATTCCCAGTAAGTGCG-3′ and 5′-GCCTCAC-TAAACCATCCAA-3′, annealing temperature 63°C. The level of gene expression was calculated by interpolation with a standard curve. cDNA copy numbers were expressed relative to 2×10^5 18s rRNA copies.

Zinc transporter silencing. CD4 T cells were transfected with 3 µg of a 1:1 mixture of two Zip6-specific siRNA (target sequences 5′-CTGGTT-GATATGGTACCTGAA-3′ and 5′-AAGGCTTATCAAGTGGTTTAA-3′; QIAGEN) by nucleofection using the Human T cell Nucleofector kit (Lonza). Control CD4 T cells were transfected with 3 µg of scrambled siRNA (QIAGEN).

After culture in RPMI/10% FCS for 48 h, knockdown efficiencies were monitored by quantitative PCR and Western blotting with rabbit anti-Zip6 serum (gift from L. Huang, Western Human Nutrition Research Center, Davis, CA). In parallel, transfected T cells were stimulated with mDC and TSST in medium supplemented with 3–60 µM zinc. Cells were examined for the expression of the activation markers CD25 and CD69 after 24 h. Zinc influx was examined by FluoZin-3 AM labeling and confocal microscopy as described in the previous section.

Phosflow. Phosphorylation status of signaling proteins was examined at a single-cell level by Phosflow as previously described (Perez et al., 2004). In brief, CD4 T cells were pelleted with 10 ng/ml TSST, 10 ng/ml SEB, and mDC in medium supplemented with different concentrations of zinc as described for the confocal studies. At indicated time points, cells were fixed with Cytofix buffer (BD) at 37°C for 10 min. Cells were permeabilized with Phosflow Perm buffer (BD) for 30 min on ice and stained with Alexa Fluor 647 anti-pZAP70 (BD) mAb. In the kinetic studies examining Lck phosphorylation, fluorescent cell barcoding was combined with Phosflow as previously described (Krutzik and Nolan 2006). PBMCs fixed at different time points after CD3 cross-linking were resuspended in permeabilizing buffer containing different concentrations of Alexa Fluor 488–NHS (N-hydroxysuccinimide; Invitrogen), incubated at room temperature for 15 min, washed, and combined before staining with PE-conjugated anti-pY505 Lck (clone 4/lck-Y505; BD) and FITC or APC–anti-CD4 mAb. Stained cells were analyzed using LSRII.

Immunoprecipitation and Western blotting. The following antibodies were used for immunoprecipitation and immunoblotting: mouse anti–human pan TCR-αβ mAb (Thermo Fisher Scientific); mouse antibody to Lck, rabbit polyclonal antibody to human TCR-β (Santa Cruz Biotechnology, Inc.); rabbit polyclonal antibody to SHP-1 (Millipore); rabbit polyclonal antibody to phosph-Src family (Tyr416), rabbit anti-Lck mAb, and phosphor ZAP70–specific antibody (Cell Signaling Technology). For pZAP70 Western blots, 30 µg of cell lysates from stimulated CD4 T cells were separated on 10% SDS-PAGE precasted gels (Bio-Rad Laboratories) under reducing conditions and transferred to polyvinylidene fluoride membrane. Membranes were blocked with 5% nonfat dried milk in 50 mM TBS, pH 7.6, with 0.1% Tween 20, incubated overnight at 4°C with anti-phospho ZAP70–specific antibody (Cell Signaling Technology), washed, and incubated with HRP-conjugated secondary antibody (Santa Cruz Biotechnology, Inc.) at room temperature for 1 h. The blot was washed thoroughly and visualized using Immobilon Western chemiluminescent detection system (Millipore). Equal loading of the samples was confirmed by stripping and reprobing the membrane for total ZAP70. For immune precipitation experiments, mature mDCs were preincubated with 10 ng/ml TSST and 10 ng/ml SEB (Toxin Technology, Inc.) for 30 min. 5×10^6 CD4 T cells were pelleted with 1×10^6 superantigen-pulsed mDCs in zinc-supplemented medium by centrifugation for 1 min at 1,350 rpm (400 g). The cells were incubated for 10 min at 37°C. Medium was removed by centrifugation. Cells were lysed in lysis buffer with 0.5% (vol/vol) Triton X-100. After 30 min on ice, lysates were cleared of debris by centrifugation for 10 min at 12,000 g and 4°C. Cell lysates were precleared by incubation for 1 h with protein A/G plus agarose (Santa Cruz Biotechnology, Inc.). Lysates were incubated for 4 h at 4°C with specific antibodies and protein A/G plus agarose, centrifuged, washed four times with cell lysis buffer, and boiled with SDS loading buffer. SDS-PAGE and immunoblotting was performed as described for ZAP70.

Statistical analysis. Data were analyzed by two-way ANOVA, with and without repeated measures, with post-hoc Tukey, or by two-sample or paired Student's t test (SigmaStat; IBM), as appropriate.

Online supplemental material. Fig. S1 shows the relationship between total and bioavailable zinc in the culture medium supplemented with ZnCl$_2$. Experiments shown in Fig. S2 demonstrate effective loading of CD4 T cell with the FluoZin-3 probe. Online supplemental material is available at http://www.jem.org/cgi/content/full/jem.20100031/DC1.

REFERENCES

Altan-Bonnet, G., and R.N. Germain. 2005. Modeling T cell antigen discrimination based on feedback control of digital ERK responses. *PLoS Biol.* 3:e356. doi:10.1371/journal.pbio.0030356

Aydemir, T.B., J.P. Liuzzi, S. McClellan, and R.J. Cousins. 2009. Zinc transporter ZIP8 (SLC39A8) and zinc influence IFN-gamma expression in activated human T cells. *J. Leukoc. Biol.* 86:337–348. doi:10.1189/jlb.1208759

Cousins, R.J., J.P. Liuzzi, and L.A. Lichten. 2006. Mammalian zinc transport, trafficking, and signals. *J. Biol. Chem.* 281:24085–24089. doi:10.1074/jbc.R600011200

Eide, D.J. 2004. The SLC39 family of metal ion transporters. *Pflugers Arch.* 447:796–800. doi:10.1007/s00424-003-1074-3

Eide, D.J. 2006. Zinc transporters and the cellular trafficking of zinc. *Biochim. Biophys. Acta.* 1763:711–722. doi:10.1016/j.bbamcr.2006.03.005

Fischer Walker, C., and R.E. Black. 2004. Zinc and the risk for infectious disease. *Annu. Rev. Nutr.* 24:255–275. doi:10.1146/annurev.nutr.23.011702.073054

Fraker, P.J., and L.E. King. 2004. Reprogramming of the immune system during zinc deficiency. *Annu. Rev. Nutr.* 24:277–298. doi:10.1146/annurev.nutr.24.012003.132454

Frederickson, C.J., J.Y. Koh, and A.I. Bush. 2005. The neurobiology of zinc in health and disease. *Nat. Rev. Neurosci.* 6:449–462. doi:10.1038/nrn1671

Haase, H., and W. Maret. 2003. Intracellular zinc fluctuations modulate protein tyrosine phosphatase activity in insulin/insulin-like growth factor-1 signaling. *Exp. Cell Res.* 291:289–298. doi:10.1016/S0014-4827(03)00406-3

Haase, H., and W. Maret. 2005. Protein tyrosine phosphatases as targets of the combined insulinomimetic effects of zinc and oxidants. *Biometals.* 18:333–338. doi:10.1007/s10534-005-3707-9

Haase, H., and L. Rink. 2009. Functional significance of zinc-related signaling pathways in immune cells. *Annu. Rev. Nutr.* 29:133–152. doi:10.1146/annurev-nutr-080508-141119

Haase, H., J.L. Ober-Blöbaum, G. Engelhardt, S. Hebel, A. Heit, H. Heine, and L. Rink. 2008a. Zinc signals are essential for lipopolysaccharide-induced signal transduction in monocytes. *J. Immunol.* 181:6491–6502.

Haase, H., S. Overbeck, and L. Rink. 2008b. Zinc supplementation for the treatment or prevention of disease: current status and future perspectives. *Exp. Gerontol.* 43:394–408. doi:10.1016/j.exger.2007.12.002

Hirano, T., M. Murakami, T. Fukada, K. Nishida, S. Yamasaki, and T. Suzuki. 2008. Roles of zinc and zinc signaling in immunity: zinc as an intracellular signaling molecule. *Adv. Immunol.* 97:149–176. doi:10.1016/S0065-2776(08)00003-5

Ho, Y., R. Samarasinghe, M.E. Knoch, M. Lewis, E. Aizenman, and D.B. DeFranco. 2008. Selective inhibition of mitogen-activated protein kinase phosphatases by zinc accounts for extracellular signal-regulated kinase 1/2-dependent oxidative neuronal cell death. *Mol. Pharmacol.* 74:1141–1151. doi:10.1124/mol.108.049064

Joazeiro, C.A., and A.M. Weissman. 2000. RING finger proteins: mediators of ubiquitin ligase activity. *Cell.* 102:549–552. doi:10.1016/S0092-8674(00)00077-5

Junttila, M.R., S.P. Li, and J. Westermarck. 2008. Phosphatase-mediated crosstalk between MAPK signaling pathways in the regulation of cell survival. *FASEB J.* 22:954–965. doi:10.1096/fj.06-7859rev

Kadrmas, J.L., and M.C. Beckerle. 2004. The LIM domain: from the cytoskeleton to the nucleus. *Nat. Rev. Mol. Cell Biol.* 5:920–931. doi:10.1038/nrm1499

Kaltenberg, J., L.M. Plum, J.L. Ober-Blöbaum, A. Hönscheid, L. Rink, and H. Haase. 2010. Zinc signals promote IL-2-dependent proliferation of T cells. *Eur. J. Immunol.* 40:1496–1503. doi:10.1002/eji.200939574

Kim, P.W., Z.Y. Sun, S.C. Blacklow, G. Wagner, and M.J. Eck. 2003. A zinc clasp structure tethers Lck to T cell coreceptors CD4 and CD8. *Science.* 301:1725–1728. doi:10.1126/science.1085643

Kitamura, H., H. Morikawa, H. Kamon, M. Iguchi, S. Hojyo, T. Fukada, S. Yamashita, T. Kaisho, S. Akira, M. Murakami, and T. Hirano. 2006. Toll-like receptor-mediated regulation of zinc homeostasis influences dendritic cell function. *Nat. Immunol.* 7:971–977. doi:10.1038/ni1373

Kröncke, K.D., L.O. Klotz, C.V. Suschek, and H. Sies. 2002. Comparing nitrosative versus oxidative stress toward zinc finger-dependent transcription. Unique role for NO. *J. Biol. Chem.* 277:13294–13301. doi:10.1074/jbc.M111216200

Krutzik, P.O., and G.P. Nolan. 2006. Fluorescent cell barcoding in flow cytometry allows high-throughput drug screening and signaling profiling. *Nat. Methods.* 3:361–368. doi:10.1038/nmeth872

Küry, S., B. Dréno, S. Bézieau, S. Giraudet, M. Kharfi, R. Kamoun, and J.P. Moisan. 2002. Identification of SLC39A4, a gene involved in acrodermatitis enteropathica. *Nat. Genet.* 31:239–240. doi:10.1038/ng913

Lee, W.W., D. Cui, M. Czesnikiewicz-Guzik, R.Z. Vencio, I. Shmulevich, A. Aderem, C.M. Weyand, and J.J. Goronzy. 2008. Age-dependent signature of metallothionein expression in primary CD4 T cell responses is due to sustained zinc signaling. *Rejuvenation Res.* 11:1001–1011. doi:10.1089/rej.2008.0747

Li, Q.J., J. Chau, P.J. Ebert, G. Sylvester, H. Min, G. Liu, R. Braich, M. Manoharan, J. Soutschek, P. Skare, et al. 2007. miR-181a is an intrinsic modulator of T cell sensitivity and selection. *Cell.* 129:147–161. doi:10.1016/j.cell.2007.03.008

Lichten, L.A., and R.J. Cousins. 2009. Mammalian zinc transporters: nutritional and physiologic regulation. *Annu. Rev. Nutr.* 29:153–176. doi:10.1146/annurev-nutr-033009-083312

Maret, W. 2006. Zinc coordination environments in proteins as redox sensors and signal transducers. *Antioxid. Redox Signal.* 8:1419–1441. doi:10.1089/ars.2006.8.1419

Maret, W., and H.H. Sandstead. 2006. Zinc requirements and the risks and benefits of zinc supplementation. *J. Trace Elem. Med. Biol.* 20:3–18. doi:10.1016/j.jtemb.2006.01.006

Mustelin, T., and P. Burn. 1993. Regulation of src family tyrosine kinases in lymphocytes. *Trends Biochem. Sci.* 18:215–220. doi:10.1016/0968-0004(93)90192-P

Mustelin, T., T. Vang, and N. Bottini. 2005. Protein tyrosine phosphatases and the immune response. *Nat. Rev. Immunol.* 5:43–57. doi:10.1038/nri1530

Nishida, K., A. Hasegawa, S. Nakae, K. Oboki, H. Saito, S. Yamasaki, and T. Hirano. 2009. Zinc transporter Znt5/Slc30a5 is required for the mast cell–mediated delayed-type allergic reaction but not the immediate-type reaction. *J. Exp. Med.* 206:1351–1364. doi:10.1084/jem.20082533

Pabo, C.O., E. Peisach, and R.A. Grant. 2001. Design and selection of novel Cys2His2 zinc finger proteins. *Annu. Rev. Biochem.* 70:313–340. doi:10.1146/annurev.biochem.70.1.313

Palacios, E.H., and A. Weiss. 2004. Function of the Src-family kinases, Lck and Fyn, in T-cell development and activation. *Oncogene.* 23:7990–8000. doi:10.1038/sj.onc.1208074

Palmiter, R.D., and L. Huang. 2004. Efflux and compartmentalization of zinc by members of the SLC30 family of solute carriers. *Pflugers Arch.* 447:744–751. doi:10.1007/s00424-003-1070-7

Perez, O.D., P.O. Krutzik, and G.P. Nolan. 2004. Flow cytometric analysis of kinase signaling cascades. *Methods Mol. Biol.* 263:67–94.

Rahmouni, S., T. Vang, A. Alonso, S. Williams, M. van Stipdonk, C. Soncini, M. Moutschen, S.P. Schoenberger, and T. Mustelin. 2005. Removal of C-terminal SRC kinase from the immune synapse by a new binding protein. *Mol. Cell. Biol.* 25:2227–2241. doi:10.1128/MCB.25.6.2227-2241.2005

Rink, L., and H. Haase. 2007. Zinc homeostasis and immunity. *Trends Immunol.* 28:1–4. doi:10.1016/j.it.2006.11.005

Sun, G., and R.J. Budde. 1999. Substitution studies of the second divalent metal cation requirement of protein tyrosine kinase CSK. *Biochemistry.* 38:5659–5665. doi:10.1021/bi982793w

Vallee, B.L., and K.H. Falchuk. 1993. The biochemical basis of zinc physiology. *Physiol. Rev.* 73:79–118.

Van Laethem, F., S.D. Sarafova, J.H. Park, X. Tai, L. Pobezinsky, T.I. Guinter, S. Adoro, A. Adams, S.O. Sharrow, L. Feigenbaum, and A. Singer. 2007. Deletion of CD4 and CD8 coreceptors permits generation of alphabetaT cells that recognize antigens independently of the MHC. *Immunity.* 27:735–750. doi:10.1016/j.immuni.2007.10.007

Yamasaki, S., K. Sakata-Sogawa, A. Hasegawa, T. Suzuki, K. Kabu, E. Sato, T. Kurosaki, S. Yamashita, M. Tokunaga, K. Nishida, and T. Hirano. 2007. Zinc is a novel intracellular second messenger. *J. Cell Biol.* 177:637–645. doi:10.1083/jcb.200702081